PROTO-PLANETARY NEBULAE

SUN KWOK
Department of Physics and Astronomy, University of Calgary, Calgary, Alberta, Canada T2N 1N4

ABSTRACT. The progress in the search for proto-planetary nebulae (PPN) in the last 5 years is reviewed. An observational definition of PPN is developed and a list of current PPN candidates is given. The optical, infrared, and radio properties of PPN are summarized and compared with theoretical models.

1. Introduction

Proto-planetary nebulae (PPN) are defined as transition objects between the end of the asymptotic giant branch (AGB) and the planetary nebulae (PN) phases (Kwok 1987). Over 1000 PN were detected in the *IRAS* survey. According to the evolutionary models of Schönberner (1983), the fraction of time a star spends in the PPN phase is ~10% of the entire PN lifetime. If this is the case, we can expect ~100 PPN candidates in the *IRAS* Point Source Catalog (PSC). PPN candidates can be identified by two ways: either by searching for stars in existing optical catalogs with appropriate *IRAS* colors, or to search for the optical counterparts of low-temperature *IRAS* sources. The PPN candidates discovered to date are the result of the combination of these two strategies.

2. Search for Proto-Planetary Nebulae

2.1. PPN CANDIDATES ASSOCIATED WITH KNOWN OPTICAL STARS

The first attempt to search the *IRAS* Point Source Catalog for associations with G-type stars was by Odenwald (1986). Excess emission was found in ~4% of the 150 G supergiants detected by *IRAS*. Several of the supergiants identified are RV Tauri variables, which have long been known to possess infrared excesses at 10 μm (Gehrz 1972). The evolutionary status of RV Tauri stars as post-AGB objects of low mass has been discussed by Jura (1986). A systematic identification of *IRAS* sources with objects with existing optical spectra has been carried out by Bidelman. Bidelman's extensive list contains several stars with intermediate spectral types (F-K) with large infrared excesses which can be candidates for PPN (Bidelman 1985).

It has been known for some time that a number of high-latitude F supergiants can be better explained as old, halo objects observed in the post-AGB phase (Bond, Carney, and Grauer 1984). Among the properties exhibited by various members of this class (but not by all) are high space

R. Weinberger and A. Acker (eds.), Planetary Nebulae, 263–270.
© 1993 *IAU. Printed in the Netherlands.*

https://doi.org/10.1017/S0074180900170998 Published online by Cambridge University Press

velocity, low metal abundance (Bond and Luck 1987), circumstellar dust (Parthasarathy and Pottasch 1986), and molecular envelopes (Likkel *et al.* 1987). The supergiant spectral classification just reflects the low gravity of these stars, but not their intrinsic luminosity. The prototype of this class of 89 Her, which is a MK spectral standard of type F2 Ia. 89 Her is located at a galactic latitude of 23°, which will put it at an unreasonably large distance above the plane if it has a luminosity of a Population I supergiant. The strongest support for its post-AGB status is the infrared excess (Gillett et al. 1970), which is likely to originate from the remnant of the CSE of its AGB progenitor.

Two other classes of variable stars are also likely to be post-AGB stars. RV Tauri stars are characterized by light curves showing alternate deep and shallow minima, with periods of 50-150 days, and have spectral type F, G, or K (Preston et al. 1963). The circumstellar envelopes of RV Tauri stars can also be seen in OH (Bujarrabal et al. 1988, Alcolea and Bujarrabal 1991) and CO. The class of UU Her stars is designated by Sasselov (1984) to represent small-amplitude variable stars of periods 40-100 days and located at high galactic latitudes. Infrared excesses similar to 89 Her have been found in RV Tauri (Gehrz 1972), but not in UU Her (Gehrz and Woolf 1970). A comprehensive study of 25 high galactic latitude supergiants with infrared excesses was made by Trams (1991).

2.2. COOL IRAS SOURCES AS PPN CANDIDATES

The search for PPN candidates by ground-based observations of *IRAS* sources satisfying certain color criteria has been carried out by several groups (Kwok 1987, van der Veen 1988, Slijkhuis 1992). Basically, candidates are selected from a certain region of the *IRAS* color-color diagram. The optical counterparts of these candidates are identified with a ground-based telescope or by positional coincidence on sky survey plates. The spectral energy distribution can be determined by visible and infrared photometry. The nature of the sources can be further defined by optical, infrared, and millimetre spectroscopy and optical/infrared imaging.

This strategy of PPN search depends critically on the correct identification of the *IRAS* sources. Many cool *IRAS* sources are evolved AGB stars which suffer from large circumstellar extinction and will not have an optically-bright counterpart (Kwok, Hrivnak, and Boreiko 1987). Identification by positional coincidence will easily lead to the wrong identification of the *IRAS* source, in particular in the Galactic plane where the field is crowded. Even when the source is identified by searching in the K band, there are still possibilities of confusion because most red stars are strong near-infrared emitters. The only sure way of obtaining the correct identification is by searching around the *IRAS* position at 10 or 20 μm and compare the observed fluxes with the *IRAS* 12 and 25 μm PSC fluxes. It is our experience that while the *IRAS* positions are generally good, there are cases where the actual source is located more than one arc min away from the PSC position.

A typical energy distribution of PPN is shown in Fig. 1. The most notable feature of a PPN is the "double-peaked" spectral distribution. The low temperature component corresponds to the remnant of the AGB envelope and the high temperature component corresponds to the reddened photosphere of the central star.

2.3. CONFUSION OF PPN WITH OTHER OBJECTS

Since there is a proliferation of the use of the term PPN in the literature, it is essential to sort out

https://doi.org/10.1017/S0074180900170998 Published online by Cambridge University Press

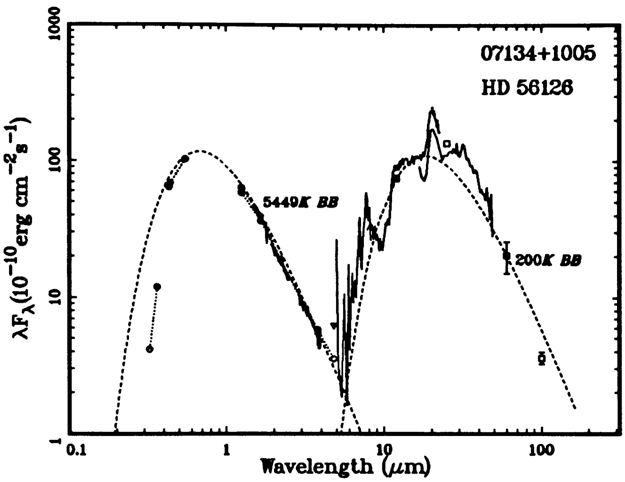

Figure 1. Spectral energy distribution of the PPN candidate 07134+1005. The solid line between 7 and 23 μm is the IRAS LRS. The H, K, and L spectra are from Kwok et al. (1990), the 5-8 μm spectrum is from Buss et al. (1990), and the 30-60 μm spectrum is from Omont et al. (1992).

which ones are real. The common causes of confusion are with: (i). PN; (ii). AGB stars; (iii). massive stars; (iv). HII regions, and (v). wrong association with the *IRAS* sources. Since PN have large far infrared excesses and often have near-infrared excesses due to nebular emission (Zhang, this volume), they are easily mistaken as PPN. Their nature can, however, be conclusively determined by optical spectroscopy or radio imaging. The difference between AGB stars and PPN is more subtle: if the two components are clearly separated, it is likely to be a PPN. AGB stars are also likely to have large-amplitude variability. As for massive stars in transition from the red to the blue, it is very difficult to separate from PPN without some independent distance estimates. For example, IRC+10420 (F8 Ia) shares many common properties with PPN but is widely believed to be a massive star.

We have developed the following observational definition for a PPN:

i. A PPN candidate should show clear evidence of the remnant of the AGB envelope. These include: (a) large infrared excess with color temperatures between 150-300 K; and (b) molecular emission (CO or OH) showing expansion velocity of 5-30 km s^{-1} typical of AGB winds.

ii. There should be evidence that the circumstellar envelope is detached from the photosphere and is not the result of an ongoing mass loss process.

iii. If the central star is bright enough for its spectral type to be determined, it should be of spectral types B-K with luminosity class I.

iv. There should not be large-amplitude photometric variability as the result of pulsation of a massive ($>10^{-3}$ $M_\odot$) hydrogen envelope above the core.

We have tabulated in Table 1 26 objects that we consider to be good candidates for PPN.

3. Optical Properties of PPN

A number of PPN candidates show emission activities in Hα. The Hα profiles range from P Cygni, inverse P-Cygni, to shell (Waters, this volume). Velocity monitoring of a number of PPN candidates have found several binary candidates (Hrivnak & Woodsworth, this volume). C_2 and C_3 molecules have been detected in a number of PPN, suggesting that these are highly carbon-rich objects (Hrivnak, this volume).

https://doi.org/10.1017/S0074180900170998 Published online by Cambridge University Press

Table 1
Proto-Planetary Nebulae Candidates

IRAS	other names	Sp. Type	l	b	Infrared	Mol. Line	Ref
04296+3429	-	G0 Ia	166.2	-9.1	21 μm	CO	a
05113+1347	-	G8 Ia	188.8	-9.1	21 μm	-	b
05381+1012	-	G	195.5	-10.6	-	-	
06530-0213	-	F0 I	215.4	-0.1	-	CO	c
07134+1005	HD 56126	F5 I	206.7	+10.0	21 μm	CO	a,d
10215-5916	DM-583221	G5: I	285.1	-1.9	silicate	-	d,h
12175-5338	SAO 239853	A9 Iab	298.3	+8.7	-	-	d
17150-3224	-	G2 I	353.8	+3.0	-	OH,CO	c,g,h
17436+5003	HD 161796	F3 Ib	77.1	+30.9	-	OH,CO	d,e
17441-2411	-	-	4.2	+2.2	-	CO	c,h
18025-3906	-	G2 I	353.3	-8.7	-	OH	c
18095+2704	-	F3 Ib	53.8	+20.2	silicate	OH	f,g
19114+0002	HD 179821	G5 Ia	36.6	-5.0	silicate	OH,CO	d,g
19454+2920	-	-	65.2	+2.1	featureless	CO	i
19475+3119	31°3797	F3 Ia	67.1	+2.7	-	CO	
19477+2401	-	-	60.8	-0.9	-	OH	i
19480+2504	-	-	61.8	-0.6	featureless	CO	
19500-1709	HD 187885	F3 I	24.0	-21.0	-	CO	d,g
20000+3239	-	G8 Ia	69.7	+1.2	21 μm	CO	b
20004+2955	V 1027 Cyg	G7 Iab	67.4	-0.4	silicate	-	d,h
20028+3910	-	-	75.5	+4.2	featureless	CO	h
22223+4327	DO 41288	G0 Ia	96.7	-11.5	21 μm	CO	
22272+5435	HD 235858	G5 Ia	103.3	-2.5	21 μm	CO	a,g,k
22574+6609	-	-	112.0	+6.0	21 μm	CO	j
23304+6147	-	G0 Ia	113.9	+0.6	21 μm	CO	a
23321+6545	-	-	115.2	+4.3	-	OH,CO	h

(a). Kwok, Volk, and Hrivnak 1989, (b). Kwok et al. 1992, (c). Slijkhuis 1992, (d). Hrivnak, Kwok, and Volk 1989, (e). Parthasarathy and Pottasch 1986, (f). Hrivnak, Kwok, and Volk 1988, (g). van der Veen 1988, (h). Volk and Kwok 1989, (i). Kwok, Hrivnak, and Boreiko 1987, (j). Hrivnak and Kwok 1991, (k). Pottasch and Parthasarathy 1988.

https://doi.org/10.1017/S0074180900170998 Published online by Cambridge University Press

4. Circumstellar Dust and Gas Features

4.1. OXYGEN-RICH PPN: SILICATES.

Since the 10 and 18 μm features of silicates are commonly observed in oxygen-rich AGB stars, it is expected that these features will also be observable in oxygen-rich PPN. It has been noted that the 10 μm feature in PPN will be much less prominent than in AGB stars because of the decline in dust temperature and the shift of the spectral peak to longer wavelengths (Kwok 1980). This effect is quantitatively confirmed by the detached-shell radiative-transfer model of Volk and Kwok (1989) who find that 10 μm feature not only weakens but also broadens. A search of the *IRAS* LRS has yielded a number of sources with the predicted shape at 10 μm (Volk and Kwok 1989). A number of these objects are later confirmed to be PPN (e.g., 18095+2704, 10215-5916, and 20004+2955). The existence of oxygen-rich PPN confirms the evolutionary connection between OH/IR stars and PN.

4.2. CARBON-RICH PPN

The dominant circumstellar dust features in carbon-rich AGB stars are SiC and (in extreme carbon stars) graphite. The strength of the 11.3 μm SiC feature is weaker than the 10 μm silicate feature, and graphite is featureless in the mid-infrared. These facts have led us to assume that carbon-rich PPN will not have strong identifying features in the 10-20 μm range. The discovery of strong emission feature at 21 μm in four PPN therefore came as a surprise (Kwok, Volk, and Hrivnak 1989). The *IRAS* LRS of these four sources show a prominent feature at 21 μm with an almost flat (in λF_λ) continuum between 12 and 18 μm. The 21 μm feature has been confirmed by both airborne (Omont et al. 1992) and ground-based observations (Barlow, this volume).

A number of suggestions have been made for the origin of this feature. Cox (1990) found similar features in a number of HII regions, and suggests that the feature is due to Fe_2O_3 or Fe_3O_4. Sourisseau et al. (1992) suggest that the 21 μm feature arises from a mixture of coal, SiC, and urea. The strength of the 21 μm feature suggests that it originates from abundant atomic species. The fact that it is associated with carbon-rich objects suggests that carbon may be a major constituent.

In addition to the well-known 3.3 μm PAH emission feature that are commonly observed in PN and HII regions, there exist emission features in the 3.4-3.5 μm region which, although present in PN, are found to be strongest in PPN (Geballe and van der Veen 1990, Geballe et al. 1992). Several identifications have been proposed for the carriers of the 3.4-3.6 μm emission features. Barker, Allamandola, & Tielens (1987) and Allamandola et al. (1989) have suggested that the 3.40 μm and 3.51 features are hot bands of the fundamental C-H vibrational stretch at 3.29 μm in PAHs. de Muizon et al. (1986) and Jourdain de Muizon, d'Hendecourt, & Geballe (1990) propose that these and other weak features are the fundamental C-H stretches of sidegroups of PAHs. They also have suggested that overtones and combinations of C-C vibrations may be responsible for the underlying plateau.

Airborne observations of two of these 21 μm sources (07134+1005 and 22272+5435) in the 5-8 μm region showed that the 6.9 and 8 μm are also present in these PPNs (Buss et al. 1990). These features closely resemble the unidentified emission bands observed in HII regions and PN. While the 3.3 and 6.2 μm features observed in HII regions and PN are thought to be fluorescently excited by UV photons, it cannot be the case in these PPN because of their late spectral types. If these bands in PPN are excited by visible photons, then the molecules responsible must be larger (>100

https://doi.org/10.1017/S0074180900170998 Published online by Cambridge University Press

C atoms) than interstellar PAH molecules (Buss et al. 1990). Based on the strength correlation between the 3.4-3.5 μm features and the 6.9 μm feature in 22272+5435, Geballe et al. suggest that the former is due to the stretching mode of CH_2 and CH_3 groups. Because of the different temperatures of the central stars in PN and PPN, the relative strengths of the 3.4-3.5 μm to the 3.3 μm features are due the different amount of UV and visible photons available.

4.3. ATOMIC AND MOLECULAR LINES

The photospheric spectrum of PPN are similar to those expected of intermediate spectral type supergiants. The infrared spectrum of F-type PPN is dominated by hydrogen absorption lines, and up to ten members of the Brackett series have been detected in one object. For PPN with spectral types later than G, the photospheric spectrum is dominated by vibrational absorption bands of CO (v=2-0 up to v=6-4). Most interestingly, CO have been observed to be in *emission* in several PPN (Hrivnak, Kwok, & Geballe, this volume).

5. Molecular Rotational Emissions

5.1. OH MASER EMISSION

While oxygen-rich AGB stars exhibit maser emissions in OH, H_2O, and SiO, not all of these emissions are expected to persist through the PPN stage. Theoretical calculations by Sun and Kwok (1987) suggest that only stars with high mass loss rates will have their 1612 MHz emission detectable through the PPN stage. An evolutionary scenario on how the strengths of these maser lines will vary after the star left the AGB is outlined by Lewis (1989). For example, the PPN 18095+2704 shows strong OH main (1665/1667 MHz) lines than the 1612 MHz line, which is usually stronger in AGB stars (Lewis, Eder, and Terzian 1990). A OH and H_2O survey of cool *IRAS* sources by Likkel (1989) have detected several PPN candidates (17436+5003, 19114+0002, 19477+2401, 23321+6545), all in the main lines.

On particular interest is the OH 1667 MHz main-line emission maser emission from 11385-5517 (HD 101584). The blue- and red-shifted components are well separated in bipolar lobes on opposite sides of the stellar position (te Lintel Hekkert et al. 1992). The measured expansion velocity increases from 9 km s^{-1} at the inner edge of each lobe to 40 km s^{-1} at the outer edge. It is likely that the OH emission occurs along the polar axis of an equatorial disk of circumstellar dust.

5.2. CO THERMAL EMISSION

Since the lower rotational transitions of the CO molecule have been detected in the circumstellar envelopes of over 200 AGB stars (Knapp and Morris 1985), it is expected that CO emission should still be detectable in PPN after the shell has detached from the photosphere. Indeed, the early candidates of PPN (e.g., AFGL 618, AFGL 2688) all show strong CO emission. CO observations of PPN have been performed by many groups, and the results are reviewed by Huggins (this volume).

The mass loss rates responsible for the creation of the remnant AGB envelope in PPN are generally estimated by applying the formula of Knapp and Morris (1985). Since the energy distributions of the PPN are well determined, the momentum flux ($\dot{M}V$) represented by the derived mass loss rates can be compared to the radiative momentum implied by total observed fluxes

https://doi.org/10.1017/S0074180900170998 Published online by Cambridge University Press

($4\pi D^2F/c$). The ratio of these two momentum fluxes is generally referred to as β (Knapp 1986). While the value of β for AGB stars are ~1, the corresponding values are higher for PPN and highest for PN (Likkel 1989; Hrivnak and Kwok 1991).

6. Morphology

Since two of the first discovered PPN candidates (AFGL 618 and AFGL 2688) show bipolar morphology, there is a great deal of interest in exploring the relationship between PPN and bipolar nebulae. Hrivnak and Kwok (1991) found that many PPN have similar spectra in the mid-infrared but have vastly different optical brightness. They interpret this discrepancy as the result of PPN with non-spherically-symmetric envelopes being viewed at different orientations. The optical bright ones are likely to be pole-on systems while optically-faint ones are edge-on. Scattered light escaping from the polar directions in edge-on systems will form a bipolar nebula in the visible. PPN candidates found to show bipolar morphology include 17150-3224 and 17441-2411 (Slijkhuis 1992; Langill et al., this volume).

7. Theoretical Models

Nebular evolution of PPN have been calculated by Volk (1992) and Szczerba (this volume). In these models, the central star evolution models of Schönberner (1983) and a variety of mass loss rates at the end of the AGB are used to calculate the dust emission spectrum at different times beyond the AGB. In the case of Volk (1992), the gas emission spectrum is calculated using the ionization model *CLOUDY* (Ferland, this volume). Tracks on the *IRAS* colour-colour diagram is also calculated by convolving the *IRAS* bandpasses with the model spectra. In order to be in agreement with the observations, Volk (1992) found that the Schönberner (1983) tracks have to be speeded up and the PPN phase does not exceed ~800 yr.

8. Conclusions

Significant progress has been made since the last IAU Symposium on Planetary Nebulae in the identification and observation of transition objects between the AGB and PN phases. Many PPN (especially the carbon-rich ones) show unique infrared properties. The detection of bipolar morphology in several PPN candidates suggests that the mass loss process in the last stages of the AGB is not entirely spherically symmetric. Most importantly, the study of PPN will give us the important clues to identify the formation mechanism of PN.

I wish to thank my collaborators Bruce Hrivnak, Kevin Volk, and C.Y. Zhang for helpful comments. This work is supported by an operating grant from the Natural Sciences and Engineering Research Council of Canada.

References

Alcolea, J., & Bujarrabal, V. 1991, *A&A*, **245**, 499
Allamandola, L.J., Tielens, A.G.G.M., & Barker, J.R. 1989, *ApJS*, **71**, 733
Barker, J.R., Allamandola, L.J., & Tielens, A.G.G.M. 1987, *APJ*, **315**, L61
Bidelman, W.P. 1985, *BAAS*, **17**, No. 4, 841
Bond, H.E., Carney, B.W., & Grauer, A.D. 1984, *PASP*, **96**, 176

https://doi.org/10.1017/S0074180900170998 Published online by Cambridge University Press

Bond, H.E., & Luck, R.E. 1987, in *The 2nd Conf. on Faint Blue Stars*, ed. A.G.D. Philips, D.S. Hayes, & J.W. Leibert (Schenectady:L.Davis), p. 527
Bujarrabal, V., Bachiller, R., Alcolea, J., & Martin-Pintado, J. 1988, *A&A*, **206**, L17
Buss, R.H. et al. 1990, *ApJ*, **365**, L23
Cox, P. 1990, *A&A*, **236**, L29
de Muizon, M., Geballe, T.R., d'Hendecourt, LB., & Baas, F. 1986, *ApJ*, **306**, L105
Geballe, T.R., & van der Veen, W.E.C.J. 1990, *A&A*, **235**, L9
Geballe, T.R., Tielens, A.G.G.M., Kwok, S., & Hrivnak, B.J. 1992, *ApJ*, **387**, L89
Gehrz, R.D. 1972, *ApJ*, **178**, 715
Gehrz, R.D., & Woolf, N.J. 1970, *ApJ*, **161**, L213
Gillett, F.C., Hyland, A.R., & Stein, W.A. 1970, *ApJ*, **162**, L21
Hrivnak, B.J., Kwok, S. 1991, *ApJ*, **368**, 564
Hrivnak, B.J., Kwok, S., & Volk, K. 1988, *ApJ*, **331**, 382
Hrivnak, B.J., Kwok, S., & Volk, K. 1989, *ApJ*, **346**, 265
Jourdain de Muizon, M., d'Hendecourt, & Geballe, T.R. 1990, in *Infrared Spectroscopy in Astronomy*, ed. B.H. Kaldeich, ESA SP-290, p. 177
Jura, M. 1986, *ApJ*, **309**, 732
Knapp, G.R. 1986, *ApJ*, **311**, 731
Knapp, G.R., & Morris, M. 1985, *ApJ*, **292**, 640
Kwok, S. 1980, *ApJ*, **236**, 592
Kwok, S. 1987, in *Late Stages of Stellar Evolution*, eds. S. Kwok & S.R. Pottasch (Reidel:Dordrecht), p. 321
Kwok, S., Hrivnak, B.J., & Boreiko, R.T. 1987, *ApJ*, **321**, 975
Kwok, S., Volk, K., & Hrivnak, B.J. 1989, *ApJ*, **345**, L51
Kwok, S., Hrivnak, B.J., & Geballe, T.R. 1990, *ApJ*, **360**, L23
Lewis, B.M. 1989, *ApJ*, **338**, 234
Lewis, B.M., Eder, J., & Terzian, Y. 1990, *ApJ*, **362**, 634
Likkel, L. 1989, *ApJ*, **344**, 350
Likkel, L., Omont, A., Morris, M., & Forveille, 1987, *A&A*, **173**, L11
Odenwald, S.F. 1986, *ApJ*, **307**, 711
Omont et al., 1992, in preparation
Parthasarathy, R., & Pottasch S.R. 1986, *A&A*, **154**, L16.
Pottasch, S.R., & Parthasarathy, M. 1988, *A&A*, **192**, 182
Preston, G.W., Krzeminski, W., Smak, J., & Williams, J.A. 1963, *ApJ*, **137**, 401
Sasselov, D.D. 1984, *Ap. Sp. Sc.*, **102**, 161
Schönberner, D. 1983, *ApJ*, **272**, 708
Slijkhuis, S. 1992, Ph.D. thesis, University of Amsterdam
Sourisseau, C., Coddens, G., & Papoular, R. 1992, *A&A*, **254**, L1
Sun, J., & Kwok, S. 1987, *A&A*, **185**, 258
te Lintel Hekkert, P., Chapman, J.M., & Zijlstra, A.A. 1992, *ApJ*, in press
Trams, N.R. 1991, Ph.D. thesis, Rijksuniversiteit Ulrecht
van der Veen, W.E.C.J. 1988, Ph.D. thesis, University of Leiden
Volk, K. 1992, *ApJS*, **80**, 347
Volk, K., & Kwok S. 1989, *ApJ*, **342**, 345

https://doi.org/10.1017/S0074180900170998 Published online by Cambridge University Press